

See discussions, stats, and author profiles for this publication at: <https://www.researchgate.net/publication/269694110>

Predominant Role of Water in Native Collagen Assembly inside Bone Matrix

ARTICLE *in* THE JOURNAL OF PHYSICAL CHEMISTRY B · DECEMBER 2014

Impact Factor: 3.3 · DOI: 10.1021/jp511288g

CITATION

1

READS

44

3 AUTHORS, INCLUDING:



Ratan Kumar Rai
University of California, San Diego

22 PUBLICATIONS 118 CITATIONS

[SEE PROFILE](#)



Chandan Singh
Centre of Biomedical Magnetic Resonance

15 PUBLICATIONS 23 CITATIONS

[SEE PROFILE](#)

Predominant Role of Water in Native Collagen Assembly inside the Bone Matrix

Ratan Kumar Rai,[†] Chandan Singh,^{†,‡} and Neeraj Sinha*,^{†,§}

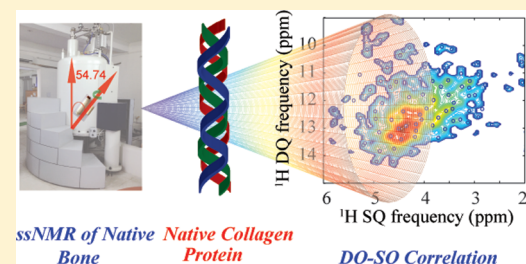
[†]Centre of Biomedical Research, SGPGIMS Campus, Raibarely Road, Lucknow 226014, India

[‡]School of Biotechnology, Banaras Hindu University, Varanasi 221005, India

Supporting Information

ABSTRACT: Bone is one of the most intriguing biomaterials found in nature consisting of bundles of collagen helices, hydroxyapatite, and water, forming an exceptionally tough, yet lightweight material. We present here an experimental tool to map water-dependent subtle changes in triple helical assembly of collagen protein in its absolute native environment. Collagen being the most abundant animal protein has been subject of several structural studies in last few decades, mostly on an extracted, overexpressed, and synthesized form of collagen protein. Our method is based on a ¹H detected solid-state nuclear magnetic resonance (ssNMR) experiment performed on native collagen protein inside intact bone matrix.

Recent development in ¹H homonuclear decoupling sequences has made it possible to observe specific atomic resolution in a large complex system. The method consists of observing a natural-abundance two-dimensional (2D) ¹H/¹³C heteronuclear correlation (HETCOR) and ¹H double quantum–single quantum (DQ-SQ) correlation ssNMR experiment. The 2D NMR experiment maps three-dimensional assembly of native collagen protein and shows that extracted form of collagen protein is significantly different from protein in the native state. The method also captures native collagen subtle changes (of the order of ~1.0 Å) due to dehydration and H/D exchange, giving an experimental tool to map small changes. The method has the potential to be of wide applicability to other collagen containing biomaterials.



1. INTRODUCTION

The structural and dynamical study of biological systems in absolute native environment is an important aspect for understanding their complete biological functions.^{1,2} However, discerning structural details in native environment is challenging. Different biological systems such as membrane proteins,^{1–3} amyloid fibrils,⁴ ion-channels,⁵ and protein complex⁶ have been studied in its native environment by solid state nuclear magnetic resonance (ssNMR) spectroscopy. Collagen is the most abundant protein of mammals, and there have been very few attempts of its structural studies in native form. Collagen protein provides mechanical stability and flexibility^{7–9} to the organism. Structural changes, mutation, and degradation of collagen protein limit the shock absorbing capacity, resulting in a serious rheumatic disease condition.^{10–12} Collagen protein forms a strong bonding with constituents such as inorganic mineral¹³ and other proteins in bones resulting in its unique mechanical and structural properties.¹⁴ Understanding the changes in collagen triple helix assembly in its true native state is important to understand its function and disease conditions as well as for the development of tissue engineering methods of artificial cartilage and bone implants.^{15,16} Collagen stability and molecular association is also governed by various water-mediated networks including hydrogen bonding,^{17–20} and these hydrogen bonds go constant rearrangement with varying hydration levels.^{21,22} Collagen and its hydration level play a major role in nucleation and deciding the shape, size,

orientation, and growth of inorganic mineral in bones.^{15,23} Recent literature suggests that water is engaged in various interactions for stabilizing bone mineral and the organic interface.^{15,23,24} These interactions work as gluing agent in bone and allow collagen with mineral particles slide without mechanical damage.²⁵ Water-mediated interaction also affects bone mechanical properties; it has been shown that dehydration and hydrogen/deuterium (H/D) exchange decreases the bone quality.^{26,27} It has been found that strength and toughness of bone decrease by almost 9% due to 5% loss of water by weight.^{27–29} Changes in collagen interaction with water are the main cause of such weakening. But these associated changes in collagen assembly are difficult to capture by spectroscopic methods. Extracted, synthetic, and over-expressed collagen protein always have different environments compared to native collagen. In this direction, ssNMR spectroscopy can provide a better probe to study collagen in its true native environment.

Recently heavy mouse (both ¹³C and ¹⁵N labeled) have been developed to refine an *in vitro* model of developing bone and to probe its detailed structure inside the bone matrix by ssNMR.³⁰ However, isotope labeling might affect the metabolic cycle and hence the biomineralization process.³⁰ Recently it has been shown that bone can also be studied with enhanced

Received: November 11, 2014

Revised: December 8, 2014

Published: December 9, 2014

sensitivity by using dynamic nuclear polarization, which have provided imino acid–aromatic interactions in native collagen without isotopic enrichments.³¹ Although there are various methods through which collagen assembly has been studied in great detail such as X-ray,^{18–20} Raman spectroscopy,^{21,22,32} FT-IR,³³ micro-CT,³³ NMR,^{13,34–42} and other biophysical methods, all of these methods have limitations to capture changes in their true native environment. Recent development in ¹H homonuclear decoupling sequences made it possible to look into atomic structural details even in large amorphous system such as peptides,^{43,44} polymers,^{45,46} and small organic molecules.^{47–50} We present here an experimental method to study native collagen protein, probing changes occurring at the lowest hierarchical level. For such measurement, we have employed ssNMR techniques to probe atomic level details ($\sim 1.0 \text{ \AA}$) in absolute native collagen. In our study, we used four kinds of intact bone collagen samples with different hydration level without any chemical treatment; three being native collagen samples with different water content (hydrated, dehydrated, and H/D exchanged) and one type 1 collagen extracted from kangaroo tail. We have applied ssNMR experiments such as windowed ¹H one-dimensional experiment (1D-DUMBO) with homonuclear decoupling (eDUMBO/DUMBO),^{51–54} ¹H–¹³C heteronuclear correlation (HETCOR),^{55–57} and 2D ¹H double quantum–single quantum (DQ-SQ) correlation^{47,58,59} to map the dipolar coupling network in native collagen protein inside bone matrix. Our results show that hydrated native collagen assembly is significantly different from extracted form of collagen protein. Analysis of 2D ¹H DQ-SQ of collagen protein spectra shows that the dipolar-coupling network gets altered due to dehydration or H/D exchanged. The change in ¹H dipolar coupling network of collagen chains suggests that triple helix undergoes rearrangement due to dehydration and H/D exchange. In case of dehydration, the ¹H–¹H dipolar coupling network becomes denser, and in the case of H/D exchange, it relaxes further as compared to native collagen. Thus, our experimental results along with simulation indicate that the method has the capability to map collagen subtle changes due to hydration and H/D exchange.

2. MATERIALS AND METHODS

2.1. Sample Preparation. For ssNMR experiments, an Indian goat (*Capra hircus*, 2–3 year old) femora bone was taken from a local slaughterhouse. The intact bone was cylindrically cut (8.0 mm long with the radius of 1.0 mm) so that it can be fixed into a 3.2 mm zirconium rotor (Supporting Figure S1). Dehydrated native collagen sample was prepared by placing bone in lyophilizer for 72 h. For H/D exchanged native collagen sample, bone was dipped into D₂O (Sigma-Aldrich USA) for 48 h to allow a maximum exchange of water present in bone with D₂O. We have also used extracted type-1 collagen purchased from Sigma-Aldrich, USA for comparative ssNMR experiments. Samples were preserved at –20 °C until experiments were performed.⁶⁰ Intact bone sample was used, as it has been reported earlier that grounding of bone disrupts internal structure.³⁸

2.2. NMR Experimental Parameters. All ssNMR spectra were recorded on 600 MHz NMR spectrometer (Avance III, Bruker Biospin, Switzerland) operating at 600.154 MHz for ¹H and 150.154 MHz for ¹³C frequencies with Bruker's 3.2 mm Efree probe. The MAS spinning speed was controlled by a Bruker's MAS pneumatic unit within an accuracy of ± 2 Hz. All one-pulse 1D, ¹H/¹³C HETCOR and 1D ¹H DUMBO,

¹H DQ-SQ 1D DUMBO ¹H DQ-SQ CRAMPS were recorded on 10.0 kHz and 12.5 kHz spinning speeds, respectively. All experiments were performed at room temperature (298 K). The pulse sequence and experimental parameters are given in Supporting Information, Figure S2 and Table S1.

2.3. Simulation Details. ¹H DQ-SQ build-up curves were simulated using SPINEVOLUTION.⁶¹ All DQ (t_1) evolution simulation was performed in one-dimensional fashion by increasing t_1 and determining ($t_2 = 0$) transverse magnetization for a single detected spin. DQ excitation and reconversions by POST C7 recoupling periods were varied systematically in simulation. Dipolar coupling interaction was turned off during the t_1 period. We have performed powder averaging by using 34 α , β , and 16 γ angles. It has been shown earlier that increasing the number of powder averaging angles does not change the shape of the simulated ¹H DQ build-up curves.⁴⁴ The default SPINEVOLUTION time step of 2 μ s was used during simulation. A total of 1024 complex time points were simulated using 80 μ s dwell time resulting total acquisition time of 82 ms. All time domain spectra were zero filled up to 16k data points with line broadening of 10 Hz prior to Fourier transformation. Time-domain output files were processed using GSim.⁶² Two PDB files have been utilized for simulation (1CAG and 1BKV). These are high-resolution-ray structures of collagen-like peptide containing single and multiple substitutions, respectively. These PDB files were used to simulate a ¹H dipolar coupling network of single and triple chain collagen protein.

2.4. Curve Fitting and Peak Picking of 2D ¹H–¹H DQ-SQ Spectra. In order to get reliable peak intensity information from overlapped 2D DQ-SQ spectrum, we used the MATLAB program (Matlab 2011(a)) to curve fit the overlapped spectra. The program automatically picks peak intensity from 2D spectra. For the curve fitting, the program utilizes peak intensity, two chemical shifts, and two line-widths (Gaussian line shape, described by their fwhm (full-width at half-maxima)). The program uses the Matlab optimization toolbox (lsqcurvefit), utilizing the trust-region-reflective fitting routine.

3. RESULTS AND DISCUSSION

According to earlier reports, dehydration and H/D exchange of bone significantly reduce its mechanical properties.^{27–29,36,64,65} The reason proposed for such weakening is mainly attributed to changes in interactions present inside collagen matrix, including hydrogen-bonding network. In order to map these changes to the lowest hierarchical level, we have carried out ssNMR experiments on bone collagen samples in native state with varying water content: hydrated native and dehydrated native collagen, H/D exchanged native collagen, and type-1 extracted collagen protein from kangaroo tail. Structural information inferred from these ssNMR spectra will map corresponding changes. Experiments were performed on intact bone samples wrapped in Teflon tape to avoid changes in water content during long NMR acquisition. One-pulse ¹H NMR spectra of hydrated native collagen recorded at MAS speed of 10 kHz are shown in Figure 1a. ¹H 1D spectrum at MAS of 10.0 kHz is dominated by peak from free water content, resonating at 5.0 ppm, and another peak at 1.4 ppm is assigned to OH[–] bound to inorganic Ca²⁺ or organic matrix.^{60,66} The resolution in the ¹H spectrum is poor to observe peaks from organic matrix, which mainly consist of collagen protein ($\sim 90\%$ of organic component in bone matrix). Changes in ¹H chemical shift should be directly correlated with corresponding changes in local environment. Recent developments in ssNMR have made it possible to

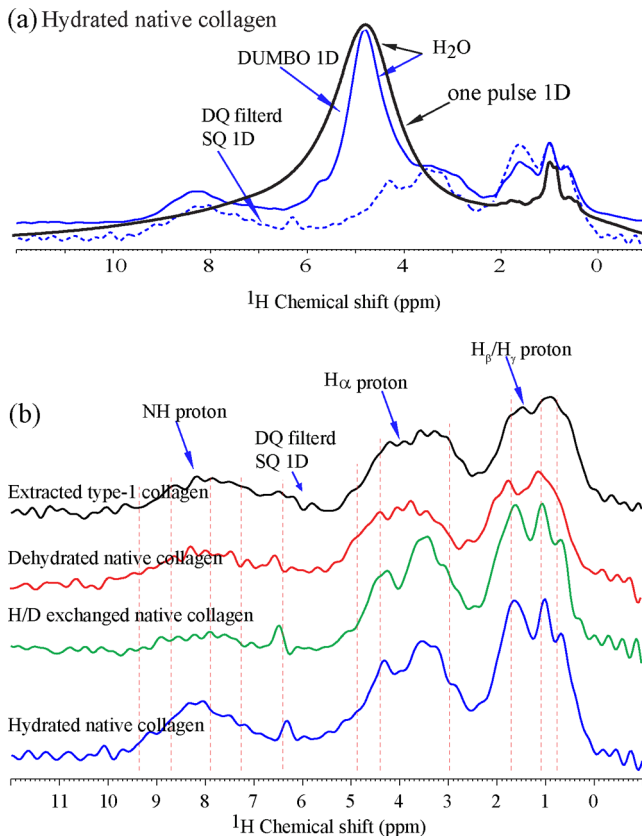


Figure 1. 1D ¹H NMR spectra of collagen (a) one-pulse ¹H NMR spectra of hydrated native collagen sample at MAS of 10 kHz (black). Comparison of DQ-SQ 1D (blue dotted) and ¹H DUMBO 1D (blue solid) of hydrated native collagen. (b) Comparison of 1D spectrum of DQ-SQ 1D spectra of extracted type-1 collagen, dehydrated, H/D exchanged, and hydrated native collagen.

observe ¹H chemical shift even at moderate MAS speed.^{57,67} Hence we recorded 1D ¹H DUMBO spectrum at moderate MAS speed (12.5 kHz). We could observe well-dispersed amide proton resonance along with aliphatic proton signals and dominant water peak, as shown in Figure 1a. DQ NMR spectroscopy can give selective information about spin pairs from dipolar-coupled network, significantly filtering free water resonance. To exclusively observe rigid dipolar coupled ¹H network, we recorded DQ filtered SQ 1D (DQ-SQ 1D) spectrum. A DQ-SQ 1D spectrum of hydrated native collagen is shown in Figure 1a. Comparing DQ-SQ 1D with DUMBO 1D, we find that free water signal at 5.0 ppm disappeared; showing ¹H resonances from relatively rigid collagen protein. If we look at the DQ-SQ 1D (Figure 1b) of different collagen samples, H_N as well as the H_α signal changes significantly among different samples, confirming participation of H_N proton in triple helical assembly through water molecules. The spectrum of hydrated native collagen is different from its extracted collagen. In the H/D exchanged native collagen sample, the H_N intensity decreases significantly; it may due to fact that the -H_N of collagen has been exchanged with deuterium.

To probe water-dependent structural changes in native collagen, we performed ¹H chemical shift assignment of all four collagen samples. The ¹H-¹³C HETCOR experiment is an effective tool to assign ¹H chemical shift of different collagen samples. Figure 2 shows the ¹H-¹³C HETCOR spectrum of different collagen samples. The ¹H and ¹³C chemical shifts have

been referenced with respect to internal reference of alanine powder packed inside MAS rotors along with collagen samples (alanine C_β ¹H/¹³C = 19.4 ppm/1.2 ppm and C_α ¹H/¹³C = 3.7 ppm/48.6 ppm). The resolution in the 2D ¹H-¹³C HETCOR spectrum is good enough to resolve ¹H chemical shift of different side chain residues of collagen. ¹³C chemical shift of collagen have been assigned by previous studies.^{38,68,69} Due to the presence of the same internal reference (alanine powder), chemical shifts from different samples can be compared. Figure 2a-d and Table 1 show a comparison of ¹H/¹³C chemical shifts of native collagen samples with different degree of water content, H/D exchange, and extracted collagen.

Change in chemical shifts is observed for all collagen samples, indicating changes in its internal structure. The Ala C_β ¹³C chemical shift is reliable indicator for probing backbone conformations due to its high sensitivity in collagen. Ala C_β resonating at 17.7 ppm in native collagen is similar to a previous study,⁶⁸ which confirms that collagen protein in bone matrix has a triple helical state. Alanine C_β changes from 17.7 to 19.0 ppm, and lines become broader and weaker in intensity due to dehydration, which shows that dehydration induces structural changes in hydrated native collagen.^{38,69} Hydrated native collagen chemical shifts are significantly different from extracted type-1 collagen. The hydrated native collagen chemical shift of Hyp C_γ, C_α, and Ala C_α is shifted to downfield compared to extracted type-1 collagen, indicating different helical packing. Similar differences in chemical shifts were also observed in case of Asp C_β ($\Delta = 0.2$), Pro C_β ($\Delta = 0.7$ ppm), Arg C_β ($\Delta = 1$ ppm), and Ala C_β ($\Delta = 2.5$ ppm), which suggest that both types of collagens are different in structure. The Ala C_β chemical shift changes from 19.9 to 17.2 ppm, which indicates that there were changes in side chain dynamics.⁶⁸ These chemical shift changes show inherent changes present in extracted type-1 collagen due to extraction. Dehydration and the H/D exchanged effect on ¹H chemical shift corresponding to few resonances are shown in Supporting Figure S3. Hydroxyproline C_γ show significant dispersion in ¹H as well as ¹³C chemical shift as a function of dehydration and H/D exchanged collagen. This confirms participation of the hydroxyl group on the hydrogen bonding network through a water molecule as ¹H ($\Delta = 0.2$ and 0.3 ppm, downfield) and ¹³C ($\Delta = 0.3$ and 0.4 ppm, up-field).⁷⁰ This change in chemical shift is observed due to rearrangement of hydrogen bonding networks.²¹ Similar changes were also observed in case of Hyp C_δ and Pro C_δ. Hyp C_δ and Pro C_δ exhibit two distinct chemical shifts in ¹H (4.0/3.5 and 3.0/3.7) as well as ¹³C (54.2, 52.3; 46.1 and 46.6), respectively. In case of H/D exchanged sample, these peaks merge into a single broad peak corresponding to Pro C_δ (¹H/¹³C = 3.3/45.6 ppm), but in the case of dehydration, it splits in two distinct peaks (¹H/¹³C = 2.7, 3.4/45.4, 46.2 ppm). We also observed changes in Hyp C_β chemical shift due to dehydration and H/D exchanged. Earlier studies indicate that Hyp and Pro are involved in pucker conformational changes in type 1 collagen.⁷¹ Changes in Hyp chemical shift show its role in fibril formation by stabilizing some Hyp in the up pucker conformation, while others are in the down conformation.⁷¹ We got similar results corresponding to the Hyp residue in the case of dehydration. The changes observed in chemical shift confirm that dehydration causes collagen structural modification. The Gly C_α peak exhibits two distinct ¹³C chemical shifts observed at 41.2 and 40.8 ppm. Gly¹H chemical shift exhibits a diastereotopic property and did not vary much due to H/D exchange and dehydration. This may be due to the fact that Gly

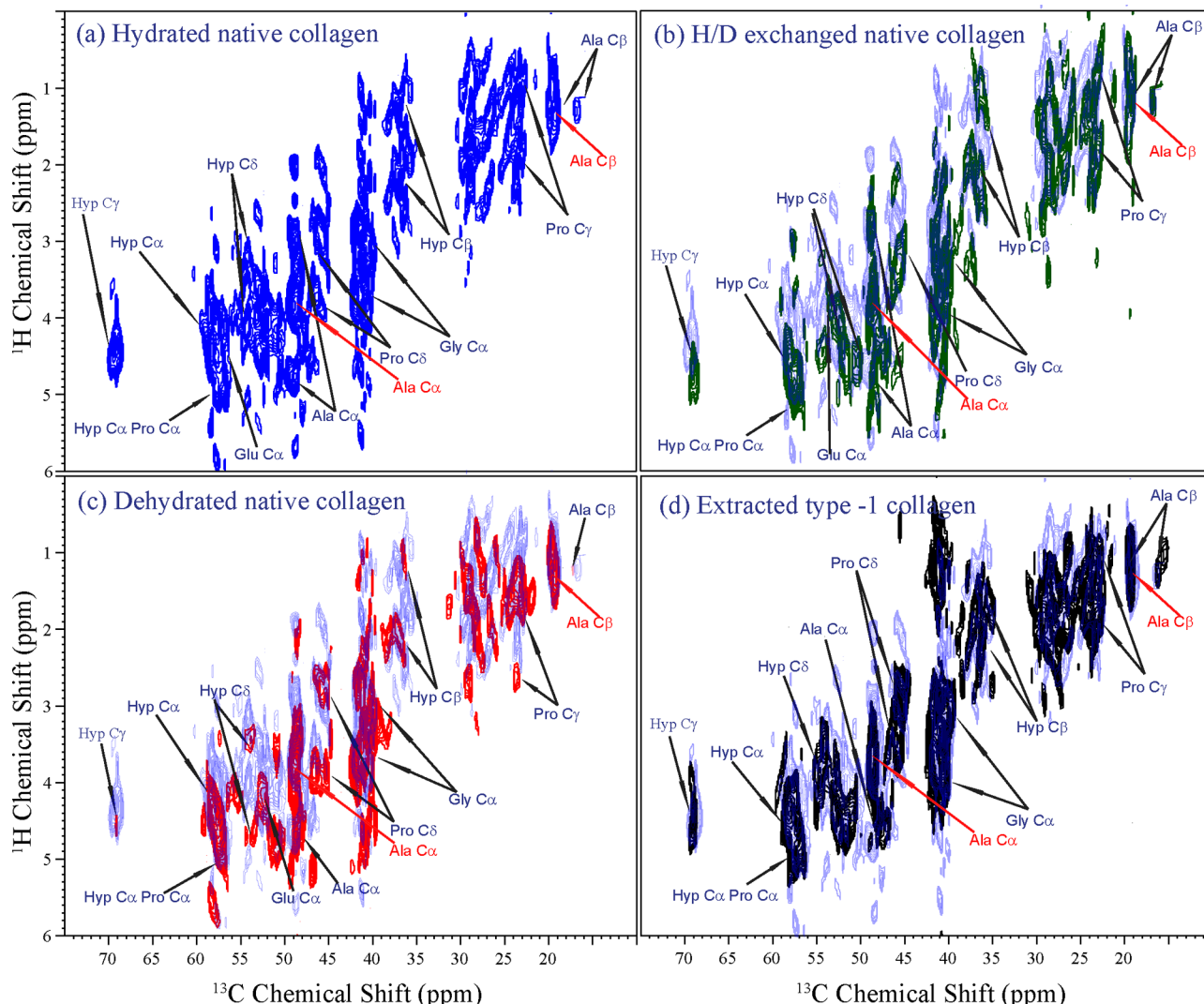


Figure 2. 2D $^1\text{H}/^{13}\text{C}$ HETCOR spectra of (a) hydrated native collagen, (b) H/D exchanged native collagen, (c) dehydrated native collagen, and (d) extracted type-1 collagen, showing the correlation of ^1H and ^{13}C chemical shifts. Assignments of various resonances are shown in the figure. Overlay spectra with a hydrated native collagen for comparison with H/D exchanged, dehydrated, extracted, and type-1 collagen are also shown in parts b, c, and d.

resides inside the triple helix core of collagen and is relatively less affected due to H/D exchange and dehydration. Another interesting observation was found in case of negatively charged amino acids such as Glu C α chemical shift. In the case of dehydration, both ^1H and ^{13}C of Glu C α shifted to upfield as compared to hydrated native collagen. This may be due to the decrease in water content of the nearby collagen helix, resulting in an increase of electron density around them. In H/D exchanged native collagen, the ^{13}C chemical shift of Glu C α changes downfield compare to hydrated native collagen. Similar changes were observed in the case of the Asp C β chemical shift, which displayed changes associated with the deprotonation effect.^{71–73} In dehydrated native collagen, these changes are due to fewer amounts of water molecules present near the collagen triple helix, which stabilizes its structure. In the case of the H/D exchanged native collagen sample, the exchange of H_2O with D_2O results in a weakened hydrogen-bonding network. Hence, we can say that $^1\text{H}/^{13}\text{C}$ HETCOR maps subtle changes in the native collagen structure due to dehydration and H/D exchange.

To probe deeper site-specific structural changes in different collagen samples, we further performed (2D) $^1\text{H}-^1\text{H}$ DQ-SQ

correlation experiments with varying POST-C7 (n_{rpl}) excitation and reconversion time. This experiment is an excellent tool to investigate different local proton dipolar coupling network environments^{43,44,46,74} and has been applied to system such as polymers,⁷⁵ peptide,⁴³ polysaccharides,⁴⁴ etc. Enhanced resolution was achieved due to the incorporation of POST-C7 and eDUMBO in 2D $^1\text{H}-^1\text{H}$ DQ-SQ correlation experiments have made it possible to study systems of a large size. We observed the line width of the order of 0.3 ppm in these spectra. The characteristic feature of 2D DQ-SQ experiments is that pairs of dipolar coupled protons DQ peaks are correlated with SQ peaks in a unique way. Peaks on diagonal appear from like spins, and on the either side of the diagonal we get symmetrically arranged peaks, which reflect a dipolar-coupling network among unlike spin. $^1\text{H}-^1\text{H}$ DQ-SQ NMR has been applied to a smaller model dipeptide to observe intra- and intermolecular short-range interaction.⁴³ In our study, we are extending the method to a larger system. $^1\text{H}-^1\text{H}$ DQ-SQ spectra (at POST-C7 reconversion/excitation block $\rightarrow n_{\text{rpl}} = 3$) of hydrated native, H/D exchanged native, dehydrated native ($n_{\text{rpl}} = 2$) and extracted type-1 collagens are shown in Figure 3.

Table 1. Assignment of $^{13}\text{C}/^1\text{H}$ NMR Spectra of the Native Collagen Sample

type of carbon	hydrated native collagen		H/D exchanged native collagen		dehydrated native collagen		type-1 extracted collagen		
	$\delta^{13}\text{C}$ (ppm) relative to alanine	δH (ppm) relative to alanine	$\delta^{13}\text{C}$ (ppm) relative to alanine	δH (ppm) relative to alanine	$\delta^{13}\text{C}$ (ppm) relative to alanine	δH (ppm) relative to alanine	$\delta^{13}\text{C}$ (ppm) relative to alanine	δH (ppm) relative to alanine	
Hyp C γ	CH	69.4	4.4	69.0	4.7	69.1	4.6	69.0	4.4
Thr C β	CH	67.2	4.2						
Pro C α	CH	58.2	4.5/5.4	58.0	4.5	59.1	4.5	58.2	4.3
Hyp C α		57.8	4.0/4.8	57.5	3.8/4.9	58.1	4.4/5.5	57.4	5.0
						55.6	4.1		
Hyp C δ	CH	54.2	4.0/3.4	54.3	3.3/4.4	53.6	3.4/4.7	54.6	4.0/3.5
Glu C α	CH	52.8	4.5	53.5	3.8	52.2	4.2	53.0	4.4
Hyp C δ	CH	52.3	4.1	52.0	4.3	51.0	3.7/4.7	51.8	4.6
Ala C α^a	CH	48.6	3.7	48.6	3.7	48.6	3.7	48.6	3.7
Ala C α	CH	48.8	4.7/3.0	48.7	4.5/5.0/3.0	48.4	4.3	47.8	4.5
Pro C δ	CH ₂	46.1/46.6	3.0/3.7	45.6	3.3	45.4/46.2	3.4/2.7	45.3	2.9
						3.8			
Gly C α	CH ₂	41.2/40.8	2.9/3.8/3.3/4.2	41.6/40.7	3.0/3.0/3.7/4.5	40.9/40.3	2.9/3.2/3.5/4.3/3.8	41.2/40.8	3.0/3.5/3.8
Arg C δ	CH ₂	40.5	3.8	39.8	3.9	39.6	4.5	39.6	4.5
Hyp C β	CH ₂	37.0	2.1/1.3	38.2	2.0	38.4	2.3	37.0	1.8
Asp C β		36.2	1.72	36.0	1.2/2.0/2.4	36.5	1.0/2.3	36.0	2.1/1.7
Pro C β ; Arg C β ;	CH ₂	29.7	1.0/2.0	29.1	1.5/2.6	31.3	1.7		
Glu C γ ; Lys C δ ;		28.8	1.4/2.2	28.5	0.9/2.1	28.9	2.7/1.5	29.0	1.9
Arg C γ		28.1	1.7	27.8	1.4	28.2	2.0/0.8	27.8	1.5/2.5
		26.9	1.5/2.4	27.2	1.7	27.3	1.4	26.6	1.9/1.0
		26.4	1.3/2.2			26.3	1.8		
Pro C γ ; Glu C β	CH ₂	25.2	1.2	26.0	1.4/2.1	25.9	0.9/2.2	24.0	1.1/1.8
		23.5	1.2/2.0	24.1	1.2	25.0	1.6	23.7	1.5
		23.1	1.6/7	23.4	1.2/1.7/2.2	23.4	1.4	23.1	1.9
				23.0	0.7/2.0	21.8	1.5		
					21.1	1.0			
Ala C β^a	CH ₃	19.4	1.2	19.4	1.2	19.4	1.2	19.4	1.2
Ala C β	CH ₃	19.9	1.0	17.7	1.1			17.2	1.0
		17.8	1.3						

^aExternally added for reference. An error of ± 0.2 ppm is expected due to line broadening in NMR spectra.

The number and pattern of DQ peaks in different collagen samples vary, showing structural changes in a broader sense. If we look at Figure 3, the region corresponding to H α –H β /H δ in 2D DQ-SQ spectrum did not show significant changes as a function of dehydration or H/D exchange. The changes due to dehydration and H/D exchange are drastic in H_N–H α regions, suggesting structural changes involving mostly amide protons of collagen. Due to the absence of amide protons in proline ($\sim 15\%$ abundance) and hydroxyproline ($\sim 14\%$ abundance) residues, these amide protons correlating with H α are corresponding to mainly glycine, alanine, lysine, arginine, threonine, and glutamine residues.⁷⁶ Since glycine is the most abundant amino acid in collagen ($\sim 26\%$), we can safely conclude that most of the resonance in 2D DQ spectrum in NH–H α region corresponds to glycine residue. We observe that number of peaks in this region increases in case of dehydration and decreases in case of H/D exchanged native collagen.

For quantification of changes in ^1H dipolar coupling network, DQ–SQ automated peak picking and fitting was performed using home written Matlab program (The Mathworks Inc.).⁷⁷ The program automatically picks peaks from 2D spectra and simulated entire spectra for accurate measurement of peak intensities and frequencies. Figure 4a shows expanded NH–H α region of 2D ^1H – ^1H DQ-SQ spectra of native collagen. Figure 4b represents the automated peak picking form experimental spectra. All selected peaks are also shown in the spectra. A simulated spectrum is shown in Figure 4c, which looks very

similar to the experimental spectra. Figure 4c shows simulated 2D spectrum along with peaks having DQ-SQ matching pairs. A complete list of all such DQ-SQ pairs for different collagen samples is given in the Supporting Information, Table S3. These DQ-SQ pairs were further used for quantification of ^1H dipolar coupling networks in different samples. We quantified dipolar-coupling network by recording 2D DQ intensity as a function of the POST-C7 (n_{rcpl}) excitation and reconversion period.⁴⁴ This was achieved by recording 2D DQ-SQ spectrum by systematically varying n_{rcpl} periods. The evolution of ^1H DQ peaks is an indicator of proton–proton proximities of dipolar-coupled network.^{44,78,79} Hence, any changes in 2D DQ-SQ evolution pattern will represent changes due to proton dipolar coupling network and will be independent of sample inhomogeneity. The buildup rate of DQ-SQ peaks will depend upon relaxation and fluctuation of local dipolar fields. The effective peak intensity can be described by an ad hoc exponential function with an effective relaxation rate t_{eff} as described earlier by Graf et al.⁸⁰

$$S_{\text{DQ}}^{ij}(t_1 = 0, t_2 = 0) \approx A(D_{ij}S_{ij})\langle q^4 \rangle t_{\text{exc}}^2 \exp\left(\frac{-t_{\text{exc}}}{t_{\text{eff}}^{ij}}\right)$$

$$\approx bt_{\text{exc}}^2 \exp\left(\frac{-t_{\text{exc}}}{t_{\text{eff}}^{ij}}\right)$$

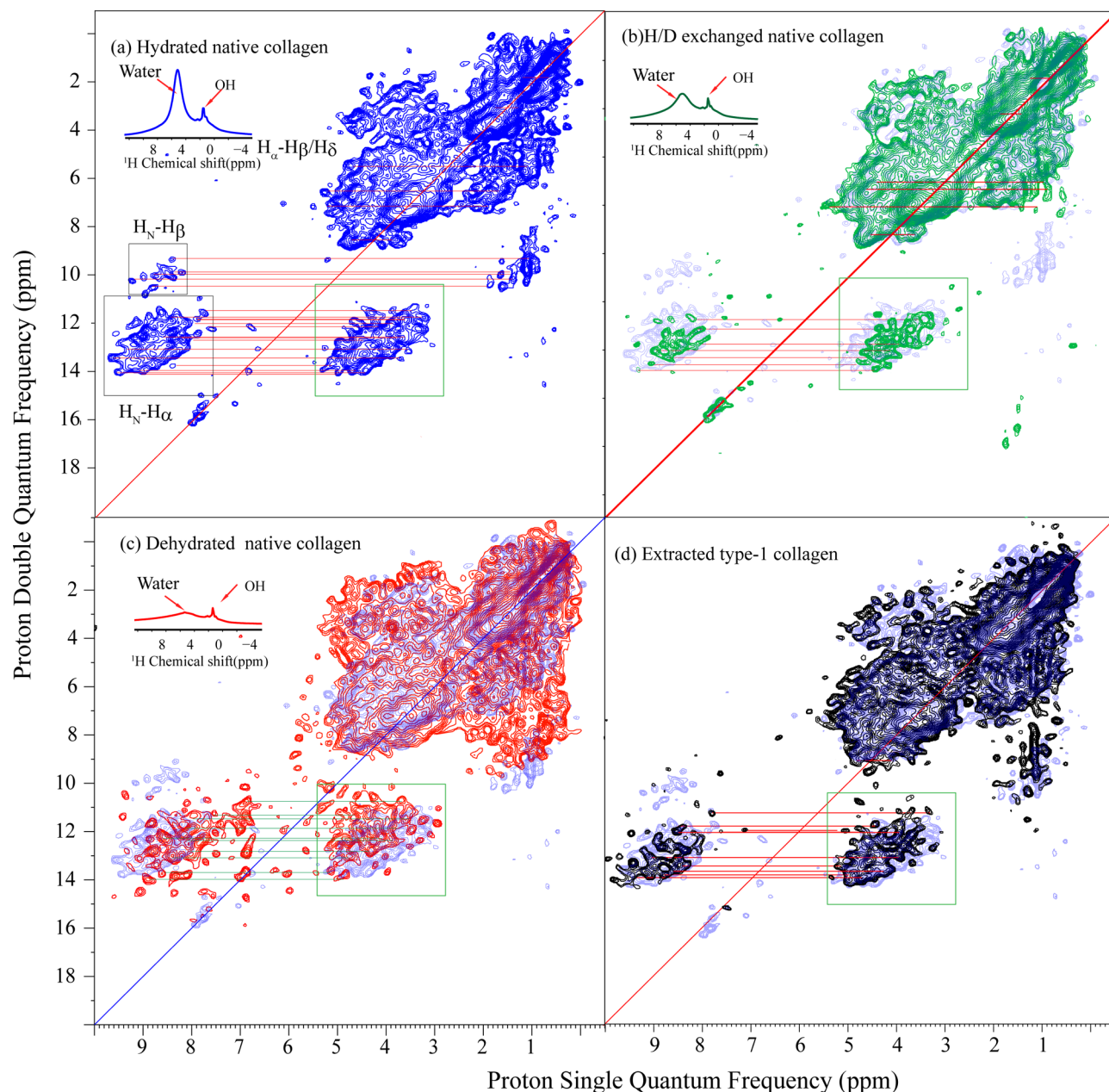


Figure 3. 2D ^1H DQ-SQ correlation spectrum of (a) hydrated native collagen, (b) H/D exchanged native collagen, (c) dehydrated native collagen, and (d) extracted type-1 collagen, showing a ^1H dipolar coupling network. The corresponding ^1H 1D spectrum showing the amount of water present in different samples is shown in the figure. Overlay spectra with hydrated native collagen for comparison with H/D exchanged, dehydrated, and type-1 collagen were also shown in parts b, c, and d.

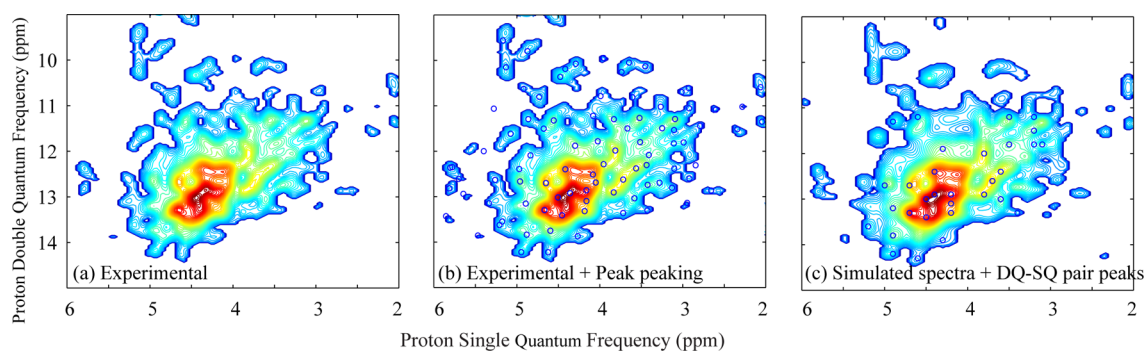


Figure 4. (a) Expanded experimental ^1H - ^1H DQ-SQ spectra of native collagen. (b) Experimental spectra of native collagen along with peak picking. (c) Simulated ^1H - ^1H DQ-SQ spectra along with selected DQ-SQ pairs.

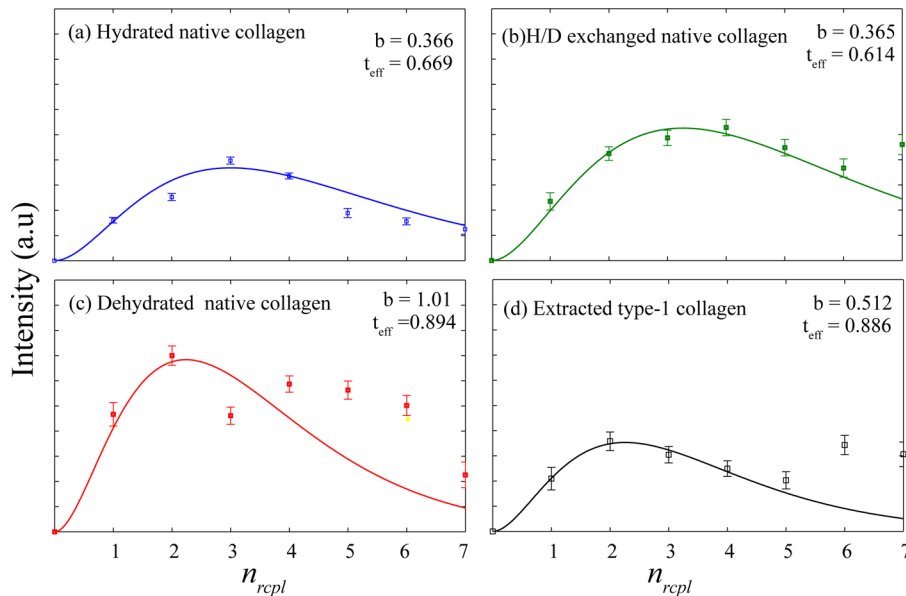


Figure 5. Experimental ^1H DQ build up intensity curve as a function of the number, n_{rcpl} , of POST-C7 elements used for the excitation and reconversion of double-quantum (DQ) coherence corresponding to various resonances in $\text{H}\alpha/\text{H}_N$ regions of (a) hydrated native collagen, (b) H/D exchanged native collagen, (c) dehydrated native collagen, and (d) extracted type-1 collagen. The figure also depicts the best fit of the experimental measured intensities (along with error bar representing signal-to-noise ratio) to the equation for the estimation of parameter b , giving an estimate of dipolar couplings.

Here A is a factor that describes the efficiency of recoupling pulse sequence and instrumental parameters, $b = A(D_{ij}S_{ij})\langle q^4 \rangle$, D_{ij} = preaveraged dipolar coupling constant, S_{ij} = order parameter, $t_{exc} = nt_R$ is the duration of the excitation or reconversion periods. Fitting the experimental DQ built-up curves for the different DQ peaks using the above equation will give an estimate of dipolar coupling (parameter b). Dipolar evolution of various peaks of native collagen as a function of n_{rcpl} are shown in Figure 5 along with the experimental signal-to-noise ratio as an error bar. The largest dipolar coupled pairs in the network govern the initial build up rate and position of maximum intensity.⁴⁴ It can be seen that evolution of peaks are different, suggesting variations in the ^1H dipolar coupling networks around $\text{H}\alpha$ corresponding to different residues. Different simulations have been performed on model collagen peptide, which indicate (Figure S4, Figure S6) that the initial buildup rate of DQ-SQ peaks depends upon strongest dipolar coupling network pair, and initial data points decide the rate of buildup curve. Hence we used initial four experimental points to fit with the above equation. The fitting of those curves will give values of parameter b , an estimate of dipolar coupling corresponding to the concerned peak. We can safely assume that dehydration did not change backbone dynamics of collagen protein as indicated by WISE experiments (Supporting Information), the parameter b will be a reliable indicator of dipolar couplings around $\text{H}\alpha$. The lower values of b will correspond to weaker dipolar coupling, while higher values of b will correspond to stronger couplings around $\text{H}\alpha$.

The changes in $\text{N}_\text{H}-\text{H}\alpha$ regions of 2D DQ-SQ spectrum corresponding to different collagen samples can be attributed to following reasons; (a) changes in backbone dynamics, where a reduction in small amplitude dynamics could decrease the motional averaging and therefore shorten T_2 and corresponding decrease in the intensity of the DQ-filtered signals, (b) dehydration introduces in-homogeneity in sample, which further causes line broadening, and (c) change in dipolar coupling network

which affect $\text{H}_N-\text{H}\alpha$ interaction due to structural changes in collagen. To rule out the possibility of disappearance of peaks in the 2D DQ spectrum due to changes in dynamics corresponding to dehydration and H/D exchange, wide line separation (WISE) experiments were also performed, and we observed that backbone dynamics does not change significantly as a function of dehydration (Figure S7).⁸¹ We got a significant change in the case of H/D exchanged bone sample for the residue Hyp C γ in which dynamics increases significantly. This may be due to the fact that Hyp C γ is involved in various hydrogen bonding networks to stabilize the chain, and the H/D exchange weakens hydrogen bonding which makes it free for segmental motion.⁴² This observation is consistent with earlier measurements of collagen side chain dynamics.⁴² Dehydration may also introduce in-homogeneity in the bone sample, and this was reported earlier that ^{13}C T_2 decreases significantly.³⁶ Similarly, we observed in the case of ^1H T_2 , which decreased DQ peak intensities due to a poor signal-to-noise ratio. To avoid this problem, we have increased the number of transients in 2D experiments for H/D exchange and dehydrated bone sample.

The distribution of b values measured from DQ-SQ evolution peaks corresponding to different collagen samples is shown in Figure 6. Since b values represent strongest dipolar coupling around $\text{H}\alpha$, it represents dipolar-coupling map of collagen protein with varying level of hydration. Each dot in the figure represents the ^1H dipolar coupling network around $\text{H}\alpha$. The dot in the figure is color-coded according to its DQ-SQ evolution pattern fit corresponding to b values. In case of hydrated native collagen, we get maximum DQ-SQ peaks corresponding to maxima at $b = 0.35$ as represented by histogram shown inset in Figure 6a.

If Gly NH is exchanged with ND, then all DQ-SQ pairs, which were excited earlier, will disappear. Similarly, DQ-SQ pairs will not be observed if all NH protons were exchanged with deuterium (Figure S5c). This explains the observation of less number of DQ-SQ peaks due to H/D exchange. If NH is

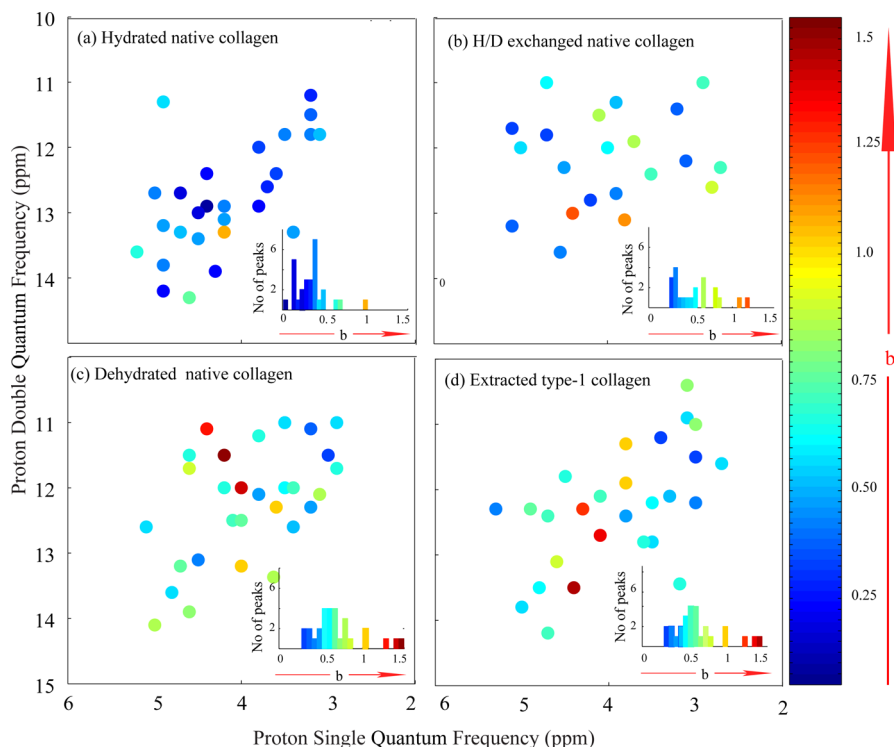


Figure 6. Dipolar coupling map of collagen triple helix inside bone matrix measured from 2D ^1H - ^1H DQ-SQ corresponding to different collagen samples. Each dot represents peaks observed in 2D DQ-SQ experiments. The color of dot represents b values measured from curve fit of the DQ-SQ build up curve, giving an estimate of dipolar couplings around $\text{H}\alpha$ corresponding to that peak. Part (a) represents hydrated native collagen; (b) H/D exchanged native collagen, (c) dehydrated native collagen, and (d) extracted type-1 collagen. The figure in inset shows distribution of b values corresponding to each sample.

exchanged with ND, it will weaken ^1H - ^1H dipolar coupling network. The DQ-SQ evolution of remaining unexchanged peaks attains maximum at b value of 0.55 (Figure 6b). This indicates that ^1H dipolar coupling network around collagen triple helix changes due to H/D exchange. For dehydrated native collagen (Figure 6c), maximum peaks attain their maxima at $b = 0.7$. This DQ-SQ evolution pattern of peaks indicate that proton dipolar-coupling network around $\text{H}\alpha$ becomes denser due to dehydration. In case of type-1 extracted collagen (Figure 6d), we find that the number of peaks and pattern is significantly different from hydrated native collagen. DQ evolution of peaks pattern suggest that we get a distribution with maximum number of peaks at $b = 0.65$ in comparison to hydrated native collagen where we attain maxima at $b = 0.35$, which suggests that extracted collagen is more compact than native collagen. This may be due to change in hydration and local environment due to the extraction of collagen from its native state.

Collagen works as a template for mineralization in bones.¹⁵ A change in collagen ^1H dipolar coupling network will be reflected due to change in the assembly, and hence it will affect the mineralization process. This method can be utilized to probe collagen changes during the mineralization process. Our experimental results can also be utilized for validating the nanomechanics of a collagen microfibril.^{25,82} These data can potentially serve as an experimental constraint for simulation to understand mechanical properties of collagen containing biomaterials.^{12,25,82} Line broadening observed in collagen resonance from various diseases such as alkaptonuria⁸³ in articular cartilage, an earlier method, failed to capture corresponding structural changes. Our method can map these changes also. This method may also be useful in case of capturing changes

due to osteogenesis-imperfect disease in which mutation in gene of collagen leads to change in hydrogen bonding network and changes in interchain distances at mutation sight.¹² Apart from these important collagen-containing systems, the method can be utilized to study cartilage, extracellular matrix (ECM), and tissue samples in its native state. This method has the potential to map assembly detail within 1 Å distance.

4. CONCLUSIONS

We have presented here method to study native collagen changes within 1 Å distances. Our study indicates that hydrated native collagen in bone matrix has entirely different ^1H - ^1H dipolar coupling network compared to extracted type-1 collagen from kangaroo tail. This consequence is due to entirely different packing of collagen triple helix. Our result indicates that the dipolar-coupling network of dehydrated collagen is denser as compared to hydrated native collagen. The method will help in understanding bone modification due to various diseases, modeling results, simulations, and energy calculations of native collagen involving water inside a triple helix,⁸⁴ the design of various scaffolds for bone implant.^{16,40,85,86} These experimental data along with simulation can be used for mimicking mechanical and ultrastructural property of bone collagen in true native state. The method presented here will be helpful in the study of abnormalities in collagen due to post-translational modification, mutation, and lathyrism. Proposed techniques can give site-specific information about changes in collagen assembly, which can further influence structural properties.¹¹ The method can also be applied to other collagen containing systems in its native state. Our results also open up new avenues for ^1H detected experiment at ultrafast MAS^{87,88} to look into collagen structure details in the native form.

■ ASSOCIATED CONTENT

§ Supporting Information

Additional experimental details and figures, as mentioned in the manuscript. This material is available free of charge via the Internet at <http://pubs.acs.org>.

■ AUTHOR INFORMATION

Corresponding Author

*E-mail: neeraj.sinha@cbmr.res.in; neerajcbmr@gmail.com.
Fax: +91-522-2668215.

Present Address

[§]Centre of Biomedical Research SGPGIMS Campus, Raibarely Road Lucknow, 226014 India.

Notes

The authors declare no competing financial interest.

■ ACKNOWLEDGMENTS

R.K.R. and C.S. acknowledge research fellowship from CSIR, India. Financial support from the Department of Biotechnology, India (Grant No. BT/PR12700/BRB/10/719/2009), is gratefully acknowledged. Author also acknowledges Dr. Vipin Agarwal (ETH, Zurich) for help in peak-picking the Matlab program and critically proof-reading the manuscript.

■ REFERENCES

- (1) Jacso, T.; Franks, W. T.; Rose, H.; Fink, U.; Broecker, J.; Keller, S.; Oschkinat, H.; Reif, B. Characterization of Membrane Proteins in Isolated Native Cellular Membranes by Dynamic Nuclear Polarization Solid-State NMR Spectroscopy without Purification and Reconstitution. *Angew. Chem., Int. Ed.* **2012**, *51*, 432–435.
- (2) Dong, H.; Sharma, M.; Zhou, H.-X.; Cross, T. A. Glycines: Role in α -Helical Membrane Protein Structures and a Potential Indicator of Native Conformation. *Biochemistry* **2012**, *51*, 4779–4789.
- (3) Cross, T. A.; Sharma, M.; Yi, M.; Zhou, H.-X. Influence of Solubilizing Environments on Membrane Protein Structures. *TIBS* **2011**, *36*, 117–125.
- (4) Tycko, R. Solid-State NMR Studies of Amyloid Fibril Structure. *Annu. Rev. Phys. Chem.* **2011**, *62*, 279–299.
- (5) Duong-Ly, K. C.; Nanda, V.; DeGrado, W. F.; Howard, K. P. The Conformation of the Pore Region of the M2 Proton Channel Depends on Lipid Bilayer Environment. *Protein Sci.* **2005**, *14*, 856–861.
- (6) Mandal, K.; Pentelute, B. L.; Tereshko, V.; Kossiakoff, A. A.; Kent, S. B. H. X-ray Structure of Native Scorpion Toxin BmBKTx1 by Racemic Protein Crystallography Using Direct Methods. *J. Am. Chem. Soc.* **2009**, *131*, 1362–1363.
- (7) Prockop, D. J.; K, K. Collagens: Molecular Biology, Diseases, and Potentials for Therapy. *Annu. Rev. Biochem.* **1995**, *64*, 403–434.
- (8) Weiner, S.; W, H. The Material Bone: Structure Mechanical Function Relations. *Annu. Rev. Mater. Sci.* **1998**, *28*, 271–298.
- (9) Shoulders, M. D.; Raines, R. T. Collagen Structure and Stability. *Annu. Rev. Biochem.* **2009**, *78*, 929–958.
- (10) Myllyharju, J.; Kivirikko, K. I. Collagens and Collagen-Related Diseases. *Ann. Med.* **2001**, *33*, 7–21.
- (11) Viguet-Carrin, S.; Garnero, P.; Delmas, P. The Role of Collagen in Bone Strength. *Osteoporosis Int.* **2006**, *17*, 319–336.
- (12) Gautieri, A.; Vesentini, S.; Redaelli, A.; Buehler, M. J. Osteogenesis Imperfecta Mutations Lead to Local Tropocollagen Unfolding and Disruption of H-Bond Network. *RSC Adv.* **2012**, *2*, 3890–3896.
- (13) Xu, J.; Zhu, P.; Gan, Z.; Sahar, N.; Tecklenburg, M.; Morris, M. D.; Kohn, D. H.; Ramamoorthy, A. Natural-Abundance ⁴³Ca Solid-State NMR Spectroscopy of Bone. *J. Am. Chem. Soc.* **2010**, *132*, 11504–11509.
- (14) Katti, D. R.; Pradhan, S. M.; Katti, K. S. Directional Dependence of Hydroxyapatite-Collagen Interactions on Mechanics of Collagen. *J. Biomech.* **2010**, *43*, 1723–1730.
- (15) Wang, Y.; Azaïs, T.; Robin, M.; Vallée, A.; Catania, C.; Legriel, P.; Pehau-Arnaudet, G.; Babonneau, F.; Giraud-Guille, M.-M.; Nassif, N. The Predominant Role of Collagen in the Nucleation, Growth, Structure and Orientation of Bone Apatite. *Nat. Mater.* **2012**, *11*, 724–733.
- (16) Penk, A.; Förster, Y.; Scheidt, H. A.; Nimptsch, A.; Hacker, M. C.; Schulz-Siegmund, M.; Ahnert, P.; Schiller, J.; Rammelt, S.; Huster, D. The Pore Size of PLGA bone Implants Determines the de Novo Formation of Bone Tissue in Tibial Head Defects in Rats. *Magn Reson Med.* **2013**, *70*, 925–935.
- (17) Bella, J.; Brodsky, B.; Berman, H. M. Disrupted Collagen Architecture in the Crystal Structure of a Triple-Helical Peptide with a Gly → Ala Substitution. *Connect. Tissue Res.* **1996**, *35*, 401–406.
- (18) Bella, J.; Berman, H. M. Crystallographic Evidence for $\text{Ca}-\text{H}\cdots\text{O}=\text{C}$ Hydrogen Bonds in a Collagen Triple Helix. *J. Mol. Biol.* **1996**, *264*, 734–742.
- (19) Bella, J.; Brodsky, B.; Berman, H. M. Hydration Structure of a Collagen Peptide. *Structure* **1995**, *3*, 893–906.
- (20) Bella, J.; Eaton, M.; Brodsky, B.; Berman, H. M. Crystal and Molecular Structure of a Collagen-Like Peptide at 1.9 Å Resolution. *Science* **1994**, *266*, 75–81.
- (21) Leikin, S.; Parsegian, V. A.; Yang, W.-H.; Walrafen, G. E. Raman Spectral Evidence for Hydration Forces Between Collagen Triple Helices. *Proc. Natl. Acad. Sci. U S A* **1997**, *94*, 11312–11317.
- (22) Leikin, S.; Rau, D. C.; Parsegian, V. A. Direct Measurement of Forces Between Self-Assembled Proteins: Temperature-Dependent Exponential Forces Between Collagen Triple helices. *Proc. Natl. Acad. Sci. U.S.A.* **1994**, *91*, 276–280.
- (23) Wang, Y.; Von Euw, S.; Fernandes, F. M.; Cassaignon, S.; Selmane, M.; Laurent, G.; Pehau-Arnaudet, G.; Coelho, C.; Bonhomme-Coury, L.; Giraud-Guille, M.-M.; Babonneau, F.; Azaïs, T.; Nassif, N. Water-Mediated Structuring of Bone Apatite. *Nat. Mater.* **2013**, *12*, 1144–1153.
- (24) Duer, M.; Veis, A. Bone Mineralization: Water Brings Order. *Nat. Mater.* **2013**, *12*, 1081–1082.
- (25) Gautieri, A.; Vesentini, S.; Redaelli, A.; Buehler, M. J. Hierarchical Structure and Nanomechanics of Collagen Microfibrils from the Atomistic Scale Up. *Nano Lett.* **2011**, *11*, 757–766.
- (26) Ong, H. H.; Wright, A. C.; Wehrli, F. W. Deuterium Nuclear Magnetic Resonance Unambiguously Quantifies Pore and Collagen-Bound Water in Cortical Bone. *J. Bone Miner. Res.* **2012**, *27*, 2573–2581.
- (27) Fernandez-Seara, M. A.; Wehrli, S. L.; Takahashi, M.; Wehrli, F. W. Water Content Measured by Proton-Deuteron Exchange NMR Predicts Bone Mineral Density and Mechanical Properties. *J. Bone. Miner. Res.* **2004**, *19*, 289–296.
- (28) Nyman, J. S.; Ni, Q.; Nicolella, D. P.; Wang, X. Measurements of Mobile and Bound Water by Nuclear Magnetic Resonance Correlate with Mechanical Properties of Bone. *Bone* **2008**, *42*, 193–199.
- (29) Nyman, J. S.; Roy, A.; Shen, X.; Acuna, R. L.; Tyler, J. H.; Wang, X. The Influence of Water Removal on the Strength and Toughness of Cortical Bone. *J. Biomech.* **2006**, *39*, 931–938.
- (30) Chow, W. Y.; Rajan, R.; Muller, K. H.; Reid, D. G.; Skepper, J. N.; Wong, W. C.; Brooks, R. A.; Green, M.; Bihani, D.; Farndale, R. W.; Slatter, D. A.; Shanahan, C. M.; Duer, M. J. NMR Spectroscopy of Native and in Vitro Tissues Implicates PolyADP Ribose in Biomineralization. *Science* **2014**, *344*, 742–746.
- (31) Singh, C.; Rai, R. K.; Aussénac, F.; Sinha, N. Direct Evidence of Imino Acid–Aromatic Interactions in Native Collagen Protein by DNP-Enhanced Solid-State NMR Spectroscopy. *J. Phys. Chem. Lett.* **2014**, *5*, 4044–4048.
- (32) Walrafen, G. E.; Chu, Y.-C. Nature of Collagen–Water Hydration Forces: a Problem in Water Structure. *Chem. Phys.* **2000**, *258*, 427–446.
- (33) Turunen, M. J.; Saarakkala, S.; Rieppo, L.; Helminen, H. J.; Jurvelin, J. S.; Isaksson, H. Comparison Between Infrared and Raman Spectroscopic Analysis of Maturing Rabbit Cortical Bone. *Appl. Spectrosc.* **2011**, *65*, 595–603.

- (34) Nikel, O.; Laurencin, D.; Bonhomme, C.; Sroga, G. E.; Besdo, S.; Lorenz, A.; Vashishth, D. Solid State NMR Investigation of Intact Human Bone Quality: Balancing Issues and Insight into the Structure at the Organic–Mineral Interface. *J. Phys. Chem. C* **2012**, *116*, 6320–6331.
- (35) Mroue, K. H.; MacKinnon, N.; Xu, J.; Zhu, P.; McNerny, E.; Kohn, D. H.; Morris, M. D.; Ramamoorthy, A. High-Resolution Structural Insights into Bone: A Solid-State NMR Relaxation Study Utilizing Paramagnetic Doping. *J. Phys. Chem. B* **2012**, *116*, 11656–11661.
- (36) Rai, R. K.; Sinha, N. Dehydration-Induced Structural Changes in the Collagen–Hydroxyapatite Interface in Bone by High-Resolution Solid-State NMR Spectroscopy. *J. Phys. Chem. C* **2011**, *115*, 14219–14227.
- (37) Rad, H. S.; Lam, S. C. B.; Magland, J. F.; Ong, H.; Li, C.; Song, H. K.; Love, J.; Wehrli, F. W. Quantifying Cortical Bone Water in Vivo by Three-Dimensional Ultra-Short Echo-Time MRI. *NMR Biomed.* **2011**, *24*, 855–864.
- (38) Zhu, P.; Xu, J.; Sahar, N.; Morris, M. D.; Kohn, D. H.; Ramamoorthy, A. Time-Resolved Dehydration-Induced Structural Changes in an Intact Bovine Cortical Bone Revealed by Solid-State NMR Spectroscopy. *J. Am. Chem. Soc.* **2009**, *131*, 17064–17065.
- (39) Best, S. M.; Duer, M. J.; Reid, D. G.; Wise, E. R.; Zou, S. Towards a Model of the Mineral–Organic Interface in Bone: NMR of the Structure of Synthetic Glycosaminoglycan- and Polyaspartate-calcium Phosphate Composites. *Magn. Reson. Chem.* **2008**, *46*, 323–329.
- (40) Weber, F.; Böhme, J.; Scheidt, H. A.; Gründer, W.; Rammelt, S.; Hacker, M.; Schulz-Siegmund, M.; Huster, D. ^{31}P and ^{13}C solid-state NMR Spectroscopy to Study Collagen Synthesis and Biomineratization in Polymer-Based Bone Implants. *NMR Biomed.* **2012**, *25*, 464–475.
- (41) deAzevedo, E. R.; Ayrosa, A. M. I. B.; Faria, G. C.; Cervantes, H. J.; Huster, D.; Bonagamba, T. J.; Pitombo, R. N. M.; Rabbani, S. R. The Effects of Anticalcification Treatments and Hydration on the Molecular Dynamics of Bovine Pericardium Collagen as Revealed by ^{13}C Solid-State NMR. *Magn. Reson. Chem.* **2010**, *48*, 704–711.
- (42) Reichert, D.; Pascui, O.; deAzevedo, E. R.; Bonagamba, T. J.; Arnold, K.; Huster, D. A Solid-State NMR Study of the Fast and Slow Dynamics of Collagen Fibrils at Varying Hydration Levels. *Magn. Reson. Chem.* **2004**, *42*, 276–284.
- (43) Brown, S. P.; Lesage, A.; Elena, B.; Emsley, L. Probing Proton–Proton Proximities in the Solid State: High-Resolution Two-Dimensional $^{1\text{H}}\text{--}^{1\text{H}}$ Double-Quantum CRAMPS NMR Spectroscopy. *J. Am. Chem. Soc.* **2004**, *126*, 13230–13231.
- (44) Bradley, J. P.; Tripion, C.; Filip, C.; Brown, S. P. Determining Relative Proton-Proton Proximities from the Build-up of Two-Dimensional Correlation Peaks in $^{1\text{H}}$ Double-Quantum MAS NMR: Insight from Multi-Spin Density-Matrix Simulations. *Phys. Chem. Chem. Phys.* **2009**, *11*, 6941–6952.
- (45) Saalwächter, K.; Lange, F.; Matyjaszewski, K.; Huang, C.-F.; Graf, R. BaBa-xy16: Robust and Broadband Homonuclear DQ Recoupling for Applications in Rigid and Soft Solids up to the Highest MAS Frequencies. *J. Magn. Reson.* **2011**, *212*, 204–215.
- (46) Saalwächter, K. Proton Multiple-Quantum NMR for the Study of Chain Dynamics and Structural Constraints in Polymeric Soft Materials. *Prog. Nucl. Magn. Reson. Spectrosc.* **2007**, *51*, 1–35.
- (47) Schnell, I.; Brown, S. P.; Low, H. Y.; Ishida, H.; Spiess, H. W. An Investigation of Hydrogen Bonding in Benzoxazine Dimers by Fast Magic-Angle Spinning and Double-Quantum $^{1\text{H}}$ NMR Spectroscopy. *J. Am. Chem. Soc.* **1998**, *120*, 11784–11795.
- (48) Brown, S. P.; Schnell, I.; Brand, J. D.; Müllen, K.; Spiess, H. W. An Investigation of π - π Packing in a Columnar Hexabenzocoronene by Fast Magic-Angle Spinning and Double-Quantum $^{1\text{H}}$ Solid-State NMR Spectroscopy. *J. Am. Chem. Soc.* **1999**, *121*, 6712–6718.
- (49) Brown, S. P.; Zhu, X. X.; Saalwächter, K.; Spiess, H. W. An Investigation of the Hydrogen-Bonding Structure in Bilirubin by $^{1\text{H}}$ Double-Quantum Magic-Angle Spinning Solid-State NMR Spectroscopy. *J. Am. Chem. Soc.* **2001**, *123*, 4275–4285.
- (50) Separovic, F.; Ashida, J.; Woolf, T.; Smith, R.; Terao, T. Determination of Chemical Shielding Tensor of an Indole Carbon and Application to Tryptophan Orientation of a Membrane Peptide. *Chem. Phys. Lett.* **1999**, *303*, 493–498.
- (51) Elena, B.; de Paëpe, G.; Emsley, L. Direct Spectral Optimisation of Proton–Proton Homonuclear Dipolar Decoupling in Solid-State NMR. *Chem. Phys. Lett.* **2004**, *398*, 532–538.
- (52) Lesage, A.; Sakellarou, D.; Hediger, S.; Eléna, B.; Charmont, P.; Steuernagel, S.; Emsley, L. Experimental Aspects of Proton NMR Spectroscopy in Solids Using Phase-Modulated Homonuclear Dipolar Decoupling. *J. Magn. Reson.* **2003**, *163*, 105–113.
- (53) Sakellarou, D.; Lesage, A.; Emsley, L. Proton–Proton Constraints in Powdered Solids from $^{1\text{H}}\text{--}^{1\text{H}}\text{--}^{1\text{H}}$ and $^{1\text{H}}\text{--}^{1\text{H}}\text{--}^{13\text{C}}$ Three-Dimensional NMR Chemical Shift Correlation Spectroscopy. *J. Am. Chem. Soc.* **2001**, *123*, 5604–5605.
- (54) Sakellarou, D.; Lesage, A.; Hodgkinson, P.; Emsley, L. Homonuclear Dipolar Decoupling in Solid-State NMR Using Continuous Phase Modulation. *Chem. Phys. Lett.* **2000**, *319*, 253–260.
- (55) Bosman, L.; Madhu, P. K.; Vega, S.; Vinogradov, E. Improvement of Homonuclear Dipolar Decoupling Sequences in Solid-State Nuclear Magnetic Resonance Utilising Radiofrequency imperfections. *J. Magn. Reson.* **2004**, *169*, 39–48.
- (56) Vinogradov, E.; Madhu, P. K.; Vega, S. Proton Spectroscopy in Solid State NMR with Windowed Phase Modulated Lee–Goldburg Decoupling Sequence. *Chem. Phys. Lett.* **2002**, *354*, 193.
- (57) Vinogradov, E.; Madhu, P. K.; Vega, S. High-Resolution Proton Solid-State NMR Spectroscopy by Phase-Modulated Lee–Goldburg Experiment. *Chem. Phys. Lett.* **1999**, *314*, 443–450.
- (58) Spiess, H. W. In *eMagRes*; John Wiley & Sons, Ltd: New York, 2007.
- (59) Schnell, I.; Spiess, H. W. High-Resolution $^{1\text{H}}$ NMR Spectroscopy in the Solid State: Very Fast Sample Rotation and Multiple-Quantum Coherences. *J. Magn. Reson.* **2001**, *151*, 153–227.
- (60) Singh, C.; Rai, R. K.; Sinha, N. Experimental Aspect of Solid-State Nuclear Magnetic Resonance Studies of Biomaterials Such as Bones. *Solid. State. Nucl. Magn. Reson.* **2013**, *54*, 18–25.
- (61) Veshtort, M.; Griffin, R. G. SPINEVOLUTION: A Powerful Tool for the Simulation of Solid and Liquid State NMR Experiments. *J. Magn. Reson.* **2006**, *178*, 248–282.
- (62) GSIM - tool for NMR spectroscopy. <http://sourceforge.net/projects/gsim/> (accessed Dec 18, 2014).
- (63) Kramer, R. Z.; Bella, J.; Mayville, P.; Brodsky, B.; Berman, H. M. Sequence Dependent Conformational Variations of Collagen Triple-Helical Structure. *Nat. Struct. Mol. Biol.* **1999**, *6*, 454–457.
- (64) Fernandez-Seara, M. A.; Wehrli, S. L.; Wehrli, F. W. Diffusion of Exchangeable Water in Cortical Bone Studied by Nuclear Magnetic Resonance. *Biophys. J.* **2002**, *82*, 522–529.
- (65) Wang, X.; Shen, X.; Li, X.; Agrawal, C. M. Age-related changes in the collagen network and toughness of bone. *Bone* **2002**, *31*, 1–7.
- (66) Wilson, E. E.; Awonusi, A.; Morris, M. D.; Kohn, D. H.; Tecklenburg, M. M.; Beck, L. W. Three Structural Roles for Water in Bone Observed by Solid-State NMR. *Biophys. J.* **2006**, *90*, 3722–3731.
- (67) Lesage, A.; Duma, L.; Sakellarou, D.; Emsley, L. Improved Resolution in Proton NMR Spectroscopy of Powdered Solids. *J. Am. Chem. Soc.* **2001**, *123*, 5747–5752.
- (68) Aliev, A. E. Solid-State NMR Studies of Collagen-Based Parchments and Gelatin. *Biopolymers* **2005**, *77*, 230–245.
- (69) Saito, H.; Tabeta, R.; Shoji, A.; Ozaki, T.; Ando, I.; Miyata, T. A High-Resolution ^{13}C -NMR Study of Collagen-like Polypeptides and Collagen Fibrils in Solid State Studied by the Cross-Polarization-Magic Angle-Spinning Method. Manifestation of Conformation-Dependent ^{13}C Chemical Shifts and Application to Conformational Characterization. *Biopolymers* **1984**, *23*, 2279–2297.
- (70) Ejchart, A. ^{13}C NMR Chemical Shifts in Aliphatic Alcohols and the γ -Shift Caused by Hydroxyl and Methyl Groups. *Org. Magn. Reson.* **1977**, *9*, 351–354.
- (71) De Sa Peixoto, P.; Laurent, G.; Azaïs, T.; Mosser, G. Solid-state NMR Study Reveals Collagen I Structural Modifications of Amino

Acid Side Chains upon Fibrillogenesis. *J. Biol. Chem.* **2013**, *288*, 7528–7535.

(72) de Dios, A. C.; Oldfield, E. Chemical Shifts of Carbonyl Carbons in Peptides and Proteins. *J. Am. Chem. Soc.* **1994**, *116*, 11485–11488.

(73) Oas, T. G.; Hartzell, C. J.; McMahon, T. J.; Drobny, G. P.; Dahlquist, F. W. The Carbonyl Carbon-13 Chemical Shift Tensors of Five Peptides Determined from Nitrogen-15 Dipole-Coupled Chemical Shift Powder Patterns. *J. Am. Chem. Soc.* **1987**, *109*, 5956–5962.

(74) Brown, S. P.; Spiess, H. W. Advanced Solid-State NMR Methods for the Elucidation of Structure and Dynamics of Molecular, Macromolecular, and Supramolecular Systems. *Chem. Rev.* **2001**, *101*, 4125–4156.

(75) Hou, S.-S.; Graf, R.; Spiess, H. W.; Kuo, P.-L. An Investigation into PEO/Crosslinked-Silicone Semi-Interpenetrating Polymer Network Using ^1H Solid-State NMR Spectroscopy under Fast MAS. *Macromol. Rapid Commun.* **2001**, *22*, 1386–1389.

(76) Eastoe, J. E. The Amino Acid Composition of Mammalian Collagen and Gelatin. *Biochem. J.* **1955**, *61*, 589–600.

(77) MathWorks. <http://www.mathworks.in/> (accessed Dec 18, 2014).

(78) Brown, S. P.; Schaller, T.; Seelbach, U. P.; Koziol, F.; Ochsenfeld, C.; Klärner, F.-G.; Spiess, H. W. Structure and Dynamics of the Host–Guest Complex of a Molecular Tweezer: Coupling Synthesis, Solid-State NMR, and Quantum-Chemical Calculations. *Angew. Chem., Int. Ed.* **2001**, *40*, 717–720.

(79) Brown, S. P.; Zhu, X. X.; Saalwächter, K.; Spiess, H. W. An Investigation of the Hydrogen-Bonding Structure in Bilirubin by ^1H Double-Quantum Magic-Angle Spinning Solid-State NMR Spectroscopy. *J. Am. Chem. Soc.* **2001**, *123*, 4275–4285.

(80) Graf, R.; Demco, D. E.; Hafner, S.; Spiess, H. W. Selective Residual Dipolar Couplings in Cross-Linked Elastomers by ^1H Double-Quantum NMR Spectroscopy. *Solid. State. Nucl. Magn. Reson.* **1998**, *12*, 139–152.

(81) Schmidt-Rohr, K.; Clauss, J.; Spiess, H. W. Correlation of Structure, Mobility, and Morphological Information in Heterogeneous Polymer Materials by Two-Dimensional Wideline-Separation NMR Spectroscopy. *Macromolecules* **1992**, *25*, 3273–3277.

(82) Launey, M. E.; Buehler, M. J.; Ritchie, R. O. On the Mechanistic Origins of Toughness in Bone. *Annu. Rev. Mater. Res.* **2010**, *40*, 25–53.

(83) Chow, W.; Taylor, A.; Reid, D.; Gallagher, J.; Duer, M. Collagen Atomic Scale Molecular Disorder in Ochronotic Cartilage from an Alkaptonuria Patient, Observed by Solid State NMR. *J. Inherit. Metab. Dis.* **2011**, *34*, 1137–1140.

(84) Landis, W. J.; Silver, F. H.; Freeman, J. W. Collagen as a Scaffold for Biomimetic Mineralization of Vertebrate Tissues. *J. Mater. Chem.* **2006**, *16*, 1495–1503.

(85) Place, E. S.; Evans, N. D.; Stevens, M. M. Complexity in Biomaterials for Tissue Engineering. *Nat. Mater.* **2009**, *8*, 457–470.

(86) Rai, R. K.; Barbhuyan, T.; Singh, C.; Mittal, M.; Khan, M. P.; Sinha, N.; Chattopadhyay, N. Total Water Phosphorus Relaxation and Inter-Atomic Organic to Inorganic Interface Are New Determinants of Trabecular Bone Integrity. *PLoS One* **2013**, *8*, e83478.

(87) Nishiyama, Y.; Zhang, R.; Ramamoorthy, A. Finite-pulse Radio Frequency Driven Recoupling with Phase Cycling for 2D $^1\text{H}/^1\text{H}$ Correlation at Ultrafast MAS Frequencies. *J. Magn. Reson.* **2014**, *243*, 25–32.

(88) Zhang, R.; Ramamoorthy, A. Performance of RINEPT is Amplified by Dipolar Couplings Under Ultrafast MAS Conditions. *J. Magn. Reson.* **2014**, *243*, 85–92.